A Machine Learning Approach to COVID-19 Detection via Graphene Field-Effect-Transistor (GFET)

Darin Tsui*, Francisco Downey*, Shreenithi Navaneethan*, Akshay Paul*, Tyler Bodily*,
Min Lee*, Yuchen Xu*, Ratnesh Lal*, and Gert Cauwenberghs*
*Shu Chien - Gene Lay Dept. of Bioengineering
University of California San Diego, La Jolla, CA 92093
Email: gcauwenberghs@ucsd.edu

***Abstract*—In the wake of the COVID-19 pandemic, there has been a need for reliable diagnostic testing. However, state-of-the-art detection methods rely on laboratory tests and also vary in accuracy. We evaluate that the usage of a graphene field-effect-transistor (GFET) coupled with machine learning can be a promising alternate diagnostic testing method. We processed the current-voltage data gathered from the GFET sensors to assess information about the presence of COVID-19 biosamples. We perform binary classification using the following machine learning algorithms: Linear Discriminant Analysis (LDA), Support Vector Machines (SVM) with the Radial Basis Function (RBF) kernel, and K-Nearest Neighbors (KNN) in conjunction with Principal Component Analysis (PCA). We find that SVM with RBF and LDA proved to be the most accurate in identifying positive and negative samples, with accuracies of 98.5% and 96.2%, respectively. Based on these results, there is promise to develop a point-of-care device for viral detection by combining GFET technology with machine learning.**

***Index Terms*—graphene field-effect-transistor, support vector machine, linear discriminant analysis, viral detection, COVID-19**

I. Introduction

Testing oneself for SARS-CoV-2 during the COVID-19 pandemic has been a crucial step toward promoting global health. The two most common state-of-the-art testing methods include laboratory reverse transcription polymerase chain reaction (RT-PCR) and rapid antigen testing [1]. However, one of the limitations of PCR testing is its reliance on centralized laboratories to get results [2]. Additionally, compared to the other methods, rapid antigen testing has a relatively high tendency to spark false negatives [3]. As such, there is a need to develop alternative methods of COVID-19 detection, such as through applications of electronics, artificial intelligence, and other indirect detection techniques.

One up-and-coming technology for COVID-19 diagnostic testing is the graphene field-effect transistor (GFET), as mentioned in a previous paper [4]. A GFET sensor utilizes an electric field to detect changes in biomolecule concentration [5]. The GFET is made up of three semiconductor devices – the source, drain, and gate. By applying a range of gate voltages, the output drain current creates a current-voltage (I-V) curve. For viral detection, the GFET is functionalized with ssDNA (single-stranded DNA) aptamers that bind to a specific target protein on the virus of interest [6]. Through this, the viral analytes bind to the aptamers located on the GFET to cause a change in drain current. However, there is limited research proving that a GFET-based system could be an automatic viral detection system. In this paper, we build on the work done in [4] and propose that interfacing a GFET system with machine learning can be an effective diagnostic testing platform for COVID-19 detection.

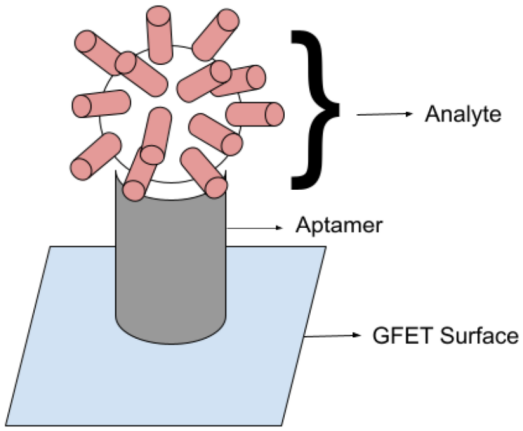

Fig. 1: Schematic diagram of the surface of a functionalized graphene field-effect-transistor (GFET) showing an aptamer with selective binding affinity to the analyte.

II. Methods

A. Preparation of GFET System

The GFET sensors were manufactured in an external facility, with the specifications detailed in [4]. The GFETs were functionalized with the aptamer for the SARS-CoV-2 nucleocapsid (N) protein. 10μL of phosphate-buffered saline (PBS) containing 1μM of the aptamer was added to the GFET chips. Fig. 1 shows a schematic diagram of a functionalized GFET.

The GFET chips were run through Fig. 2 to obtain their I-V curves. To collect data, a connection from the Keithley source measuring unit (SMU) to the GFET sensor was accomplished by ensuring metal contact with the three GFET sensor pins. The drain-source voltage (V_{DS}) was fixed at 100mV while the gate-source voltage (V_{GS}) was swept through the values from -0.5V to +0.5V [4]. Voltage was swept between these values in the positive direction (from -0.5 V to +0.5 V), which we will refer to as a forward sweep, and then in the negative direction (from +0.5 V to -0.5 V), which we will refer to as a backward sweep. This forward/backward sweep sequence was carried out four times (4 forward and 4 backward sweeps total). The drain-to-source current (I_{DS}) was recorded to create the I-V characteristic curve from the V_{GS} voltage sweep. The I-V curve illustrates the Dirac point (global minimum of the I-V curve) of each sweep, which has been used extensively as an indicator of aptamer-target binding events.

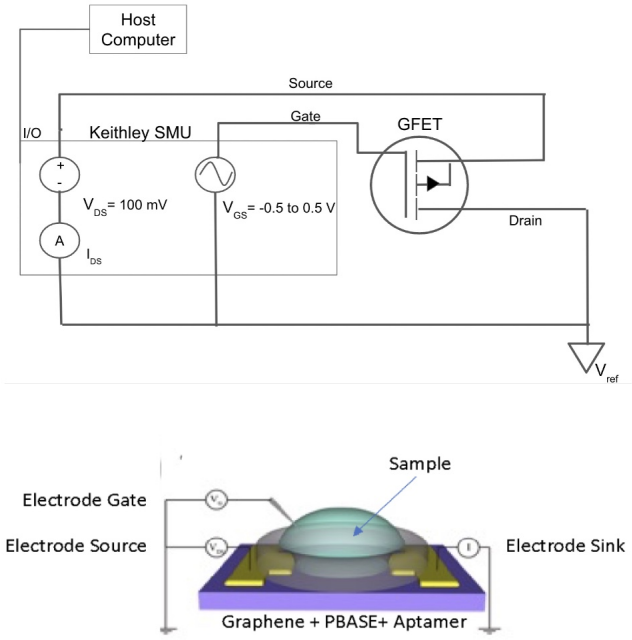

Fig. 2: Instrumentation diagram (above) of the GFET measurement depicts a computer-controlled dual-channel source meter (Keithley) driving the V_{GS} waveform while simultaneously recording the I_{DS} signal. A 3-dimensional rendering (below) of the functionalized GFET sensor chip with applied test sample and signal connections corresponding to instrumentation schematic. [4]

B. Data Collection

To explore machine learning methods for differentiating between viral and non-viral samples, we obtained the I-V curves for 19 test samples. 9 of the samples contained the Omicron strain of COVID-19, and will be referred to as the positive samples. The 10 negative samples contain no traces of COVID-19. The data collected for this machine learning analysis was taken in part from previous work done at the University of California San Diego [4].

Before adding the samples, 0.1X PBS was added to the GFETs and ran through the GFET interface shown in Fig. 2 to obtain their I-V curves. This initial curve generation will be defined as the baseline run. The saliva-virus samples were then added to the GFET, and after a few minutes of incubation for aptamer-target binding, the I-V curves were obtained. This will be defined as the sample run.

I-V curves were generated for all 19 samples to obtain their baseline and sample runs. 1000 I-V points were collected from each run on a GFET sensor. Here, each run was comprised of 8 voltage sweeps (4 forward sweeps and 4 backward sweeps, as mentioned in *Preparation of GFET System*).

The data being used was derived from each GFET sensor configured with either the Keithely SMU or the PIVOT, a handheld device that can run the GFET sensor and output the curves [4]. The data includes outputs from both baseline and sample runs for the given sensor. All the positive samples used in this study were run on GFET sensors that were functionalized with an aptamer for the Omicron variant of COVID-19.

C. Pre-processing and Feature Extraction

Upon obtaining the I-V curves, we separated them into forward and backward sweeps. For each sweep, we created two feature spaces to be used for the machine learning portion.

The first feature space, which we will refer to as the Dirac Set, involves finding the I-V point that corresponds with the Dirac point of each sweep. To create the Dirac Set, we took the Dirac point of a single baseline sweep as well as the Dirac point of a single sample sweep from the same chip and experimental test. We used these two Dirac points to create a 4-dimensional feature space. These 4 dimensions are the voltage corresponding to the baseline Dirac point, the voltage corresponding to the sample Dirac point, the current corresponding to the baseline Dirac point, and the current corresponding to the sample Dirac point.

The second feature space, which we will refer to as Curve Estimation Set, also involves finding the Dirac point of the sweeps, as well as taking 4 evenly spaced I-V points between the Dirac point and each end of the curve (9 points total). We used these spaced-out points to create a 36-dimensional feature space (9 points multiplied by the same 4 dimensions mentioned in the previous feature space). Fig. 3 displays the processing pipelines for both feature sets.

D. Model Training and Testing

We trained and tested three different models using our two feature sets to explore the possibility of classifying positive and negative samples based on GFET curves. The three models that were trained and tested on in this paper include Linear Discriminant Analysis (LDA), Support Vector Machine with the Radial Basis Function (RBF) kernel, and K-Nearest Neighbors (KNN) with Principal Component

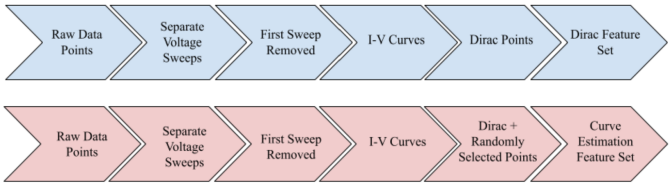

Fig. 3: Processing pipeline of Dirac and Curve Estimation Feature Sets.

Analysis (PCA). We tested these models using ten-fold cross-validation. We report accuracy, precision, and recall for all of the models.

III. Results

A. Visual Inspection of I-V Samples

Given that the machine learning results returned high accuracies, we looked to visualize our results. Fig. 4 illustrates the visual differences between negative and positive samples. We plotted the entire run of one of the negative and positive samples. It can be seen that the baseline and sample sweep in the negative case overlaps with each other. However, there appears to be a horizontal shifting of the sample sweep from the baseline sweep in the positive case. This change makes sense in the positive case since the addition of the COVID-19 biosample modulates the transfer of charges across the graphene.

Classical methods of GFET curve classification involve analyzing the absolute value of the Dirac voltage difference between the baseline and sample curves. From there, a linear decision boundary is formed for the classification between positive and negative samples. To visually compare classical methods of GFET classification to machine learning-based ones, we analyzed one testing fold of our testing data and manually classified the samples as positive and negative. Fig. 5 displays the manual decision boundary created that maximizes the testing accuracy. Using this method, we were able to get an accuracy of 68.4%.

Fig. 6 displays one testing fold of the class labels that LDA predicts for the Dirac Set and Curve Estimation Set, respectively. We plot only the Dirac points of the sample curve along their linear discriminant. Here, we are able to see a clear separation between positive and negative samples.

B. Performance of Machine Learning Models

Table I reports the accuracy, precision, and recall from the Dirac Feature Set. Table II reports the accuracy, precision, and recall from the Curve Estimation Feature Set.

TABLE I: Accuracy, precision, and recall reporting for Dirac Feature Set using different classifiers.

Classifiers	Accuracy	Precision	Recall
LDA	0.657	0.499	0.688
SVM and RBF	0.985	0.967	1.000
PCA + KNN	0.951	0.897	1.000

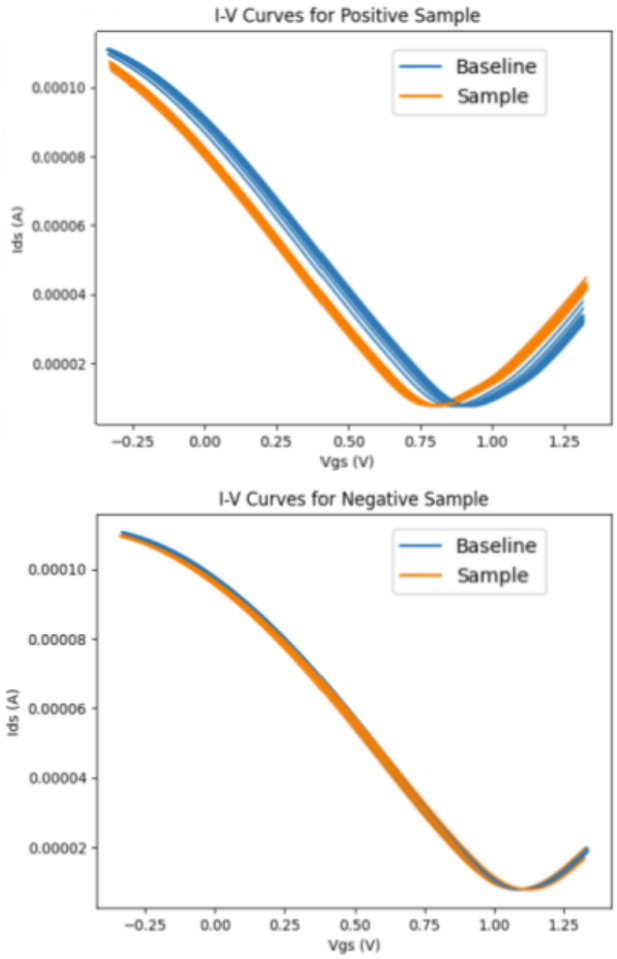

Fig. 4: I-V curves from a single run of a positive sample (above) and a negative control sample (below) applied to the GFET sensor.

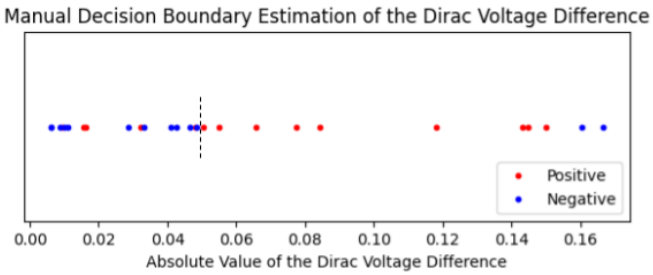

Fig. 5: Manual classification of the absolute value of the Dirac voltage differences between the baseline and sample runs.

TABLE II: Accuracy, precision, and recall reporting for Curve Estimation Feature Set using different classifiers.

Classifiers	Accuracy	Precision	Recall
LDA	0.962	0.935	0.986
SVM and RBF	0.928	0.848	1.000
PCA + KNN	0.934	0.892	0.967

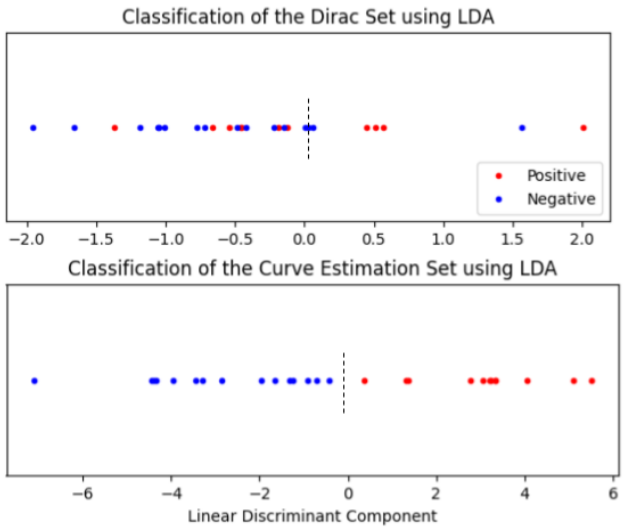

Fig. 6: Classifications of the Dirac and Curve Estimation Sets using LDA.

It can be seen in Table I that SVM with RBF recorded the highest accuracy using the Dirac Feature Set at 98.5%. In Table II, LDA recorded the highest accuracy using the Curve Estimation Feature Set at 96.2%.

IV. Discussion

A. Viral Sample Classification

When using LDA, accuracy, precision, and recall all significantly improved as a result of adding additional points to characterize the curves rather than just the Dirac points. This was most likely because LDA assumes that the given classes are linearly separable, and performance generally improves upon inputting additional data [7]. Additionally, using the Dirac Set, SVM interfaced with RBF performed the best. This is most likely because by fitting a nonlinear decision boundary, we were able to increase the complexity of our model to accommodate the limited feature space [8].

Despite the limited dataset used, the high accuracy, precision, and recall scores achieved in both feature sets suggest that GFET chips interfaced with machine learning could be a promising pipeline for effective COVID-19 diagnostic testing. With further optimization, it may be possible to develop a multi-class classification model that is able to detect distinct mutations in a virus using a single aptamer or detect entirely different viruses besides COVID.

B. Potential for Sensor Optimization

In addition to further studying the use of machine learning methods for more robust results classification, optimizing the sensor itself could result in improving the performance of the device. Increasing accuracy, speed, and sensitivity of the GFET system would allow for the creation of a more portable, point-of-care device that could be used for diagnostic testing. However, efforts towards this goal would involve decreasing power consumption and memory usage for such a device to be feasible. Some parameters that could potentially be optimized include minimizing the amount of voltage V_{DS} is clamped at, as well as adjusting the type of waveform fed into V_{GS}.

V. Conclusion

In this study, we have shown that GFET sensors interfaced with machine learning have promising potential for effective COVID-19 detection. We performed binary classification on samples that were positive and negative for COVID-19 using current-voltage data generated from the GFETs on the following algorithms: Linear Discriminant Analysis (LDA), Support Vector Machine (SVM) with the Radial Basis Function (RBF) kernel, and K-Nearest-Neighbors (KNN) with Principal Component Analysis (PCA). We find that using SVM with RBF as well as LDA achieved accuracies of 98.5% and 96.2%, respectively. Future work will be devoted to optimizing the GFET sensor, as well as exploring multi-class classification of different viral mutations for use in portable devices.

Acknowledgment

The authors of this paper would like to thank members of the Integrated Systems Neuroengineering Lab and the Lab for Nano-bio-imaging and Devices in the Shu Chien - Gene Lay Department of Bioengineering, as well as the University of California San Diego Bioengineering Senior Design program's professor Dr. Bruce Wheeler and teaching assistant Anahid Foroughishafiei for all their support and guidance.

References

[1] B. Giri, S. Pandey, R. Shrestha, K. Pokharel, F. S. Ligler, and B. B. Neupane, "Review of analytical performance of COVID-19 detection methods," Analytical and Bioanalytical Chemistry, Sep. 2020, doi: https://doi.org/10.1007/s00216-020-02889-x.

[2] A. Afzal, "Molecular diagnostic technologies for COVID-19: Limitations and challenges," Journal of Advanced Research, vol. 26, pp. 149–159, Aug. 2020, doi: https://doi.org/10.1016/j.jare.2020.08.002.

[3] G. Liu and J. F. Rusling, "COVID-19 Antibody Tests and Their Limitations," ACS Sensors, vol. 6, no. 3, pp. 593–612, Feb. 2021, doi: https://doi.org/10.1021/acssensors.0c02621.

[4] D. K. Ban et al., "Rapid self-test of unprocessed viruses of SARS-CoV-2 and its variants in saliva by portable wireless graphene biosensor," Proceedings of the National Academy of Sciences, vol. 119, no. 28, Jun. 2022, doi: https://doi.org/10.1073/pnas.2206521119.

[5] G. Seo et al., "Rapid Detection of COVID-19 Causative Virus (SARS-CoV-2) in Human Nasopharyngeal Swab Specimens Using Field-Effect Transistor-Based Biosensor," ACS Nano, vol. 14, no. 4, pp. 5135–5142, Apr. 2020, doi: https://doi.org/10.1021/acsnano.0c02823.

[6] J. Sengupta and C. M. Hussain, "Graphene-based field-effect transistor biosensors for the rapid detection and analysis of viruses: A perspective in view of COVID-19," Carbon Trends, p. 100011, Dec. 2020, doi: https://doi.org/10.1016/j.cartre.2020.100011.

[7] G. James, D. Witten, T. Hastie, and R. Tibshirani, in An introduction to statistical learning: With applications in R, Boston: Springer, 2022, pp. 152–153.

[8] K. Tbarki, S. Ben Said, R. Ksantini, and Z. Lachiri, "RBF kernel based SVM classification for landmine detection and discrimination," IEEE Xplore, Nov. 01, 2016. https://ieeexplore.ieee.org/abstract/document/7880146.